Environmental Science & Technology
June 2016, Volume 50, Issue 15, Pages 8188-8195
http://dx.doi.org/10.1021/acs.est.6b00187
http://archimer.ifremer.fr/doc/00344/45510/

Simultaneous nitrite/nitrate imagery at millimeter scale through the water-sediment interface

Metzger Edouard [1, *], Thibault Aubin [1, 2], Cesbron Florian [1, 3], Barbe Anthony [1], Launeau Patrick [4], Jezequel Didier [5], Mouret Aurélia [1]

[1] Université d'Angers, LPG-BIAF, UMR CNRS 6112, 49045 Angers Cedex, France
[2] Ifremer, LBCM, Rue de l'Ile d'Yeu, 44300 Nantes, France
[3] University of West Florida, CEDB, 11000 University Parkway, Pensacola, FL 32514 ,USA
[4] Université de Nantes, LPG-N, UMR CNRS 6112, 44322 Nantes, France
[5] Institut de Physique du Globe de Paris, Sorbonne Paris Cité, Univ. Paris Diderot, UMR 7154 CNRS, 75005 Paris, France

* Corresponding author : Edouard Metzger, +33(0)2 41 73 53 82. ; Fax: +33(0)2 41 73 53 52. ; email address : edouard.metzger@univangers.fr

Abstract :

The present study describes new procedures to obtain at millimeter resolution the spatial distribution of nitrite and nitrate in porewaters, combining diffusive equilibrium in thin films (DET), colorimetry and hyperspectral imagery. Nitrite distribution can be easily achieved by adapting the well-known colorimetric method from Griess (1879) and using a common flatbed scanner with a limit of detection about 1.7 µmol L-1. Nitrate distribution can be obtained after reduction into nitrite by a vanadium chloride reagent. However, the concentration of vanadium chloride used in this protocol brings coloration with a wide spectral signature that creates interference only deconvolvable by imaging treatment from an entire visible spectrum for each pixel (spectral analysis). This can be achieved by hyperspectral imaging. The protocol retained in the present study allows obtaining a nitrite/nitrate image with micromolar limit of detection. The methods were applied in sediments from the Loire Estuary after different treatments and allowed to precisely describe two-dimensional millimeter features. The present technique adds to the combination of gel-colorimetry and hyperspectral imagery a very promising new application of wide interest for environmental issues in the context of early diagenesis and benthic fluxes.

Graphical abstract :

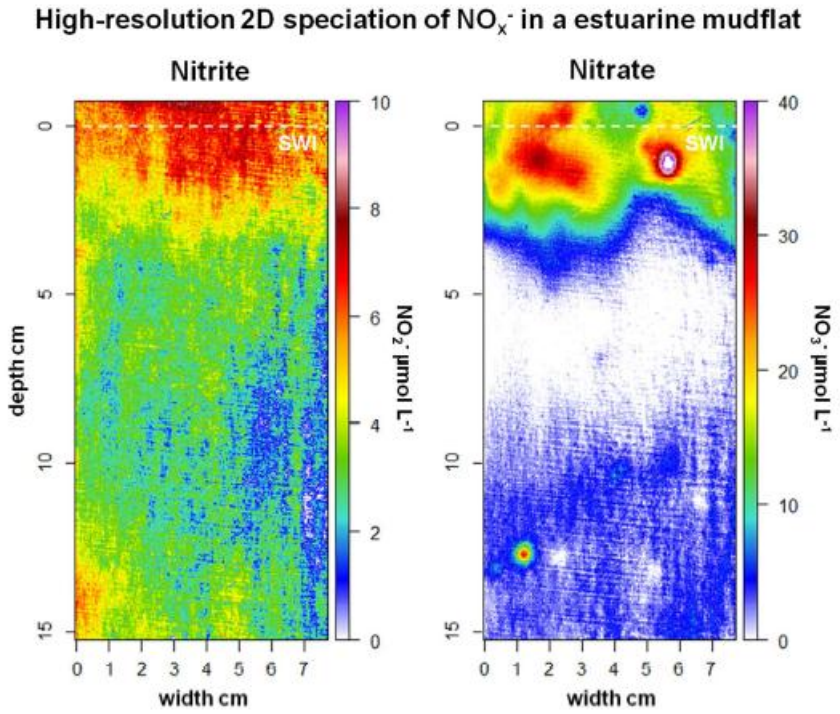

1. Introduction

Combination of diffusive equilibrium in thin film gel techniques (DET),[1] and spectrophotometry allows theoretically to reach speciation of nutrients, completing the set of tools existing for porewater chemistry at millimeter and sub-millimeter resolution. However, the main limitation of the combination of colorimetry and gel techniques is the limit of detection (LOD) induced by very small samples (below 100 µL) and subsequent dilution that is required to get sufficient volume for analytical purposes. [2–4] Only miniaturization and sensibility increase of analytical devices permit to overcome this limitation (*e.g.*: Nanodrop coupled with microplates). This is why most studies combine DET gel sampling with total elementary analyses such as ICP-MS or GF-AAS. [5] Few studies have combined DET sampling with ion chromatography to determine sulfate and nitrate concentrations.[6–8] In these works, the gel of the DET probe was cut into strips corresponding to a resolution of 2 to 20 mm. This generated at lot of samples to process and represents a time-consuming method, to finally obtain a 1D profile with a rather low resolution. Another alternative to remove such limitation was to generate an image of the distribution of dissolved compounds within the gel by direct contact of the DET gel with a reagent, either contained in another reactive gel [9,10] or in a solution. [11] Although simple and fast this approach has an important limitation in the case of slow color development: (1) a rapid and uncontrolled back-diffusion of chemicals into the reagent gel or solution, before coloring reaction, combined with lateral diffusion within the probe gel, that forbids any modeling for recalculation of 2D features using kinetics-transport modeling. [9,10] Such limitation is less important for fast-kinetic reactions such as for iron and alkalinity, which develop coloration in a short time (<1 min.); (2) a need for a rapid processing that generates important handling, forbids postponing analysis and limits the number of probes to be processed. Recent studies [12,13] showed the possibility to freeze gel probes allowing further analysis and almost no limit to the number of probe deployment. However, the major input of these studies was the use of a hyperspectral camera allowing a

48 better sensitivity and a higher spectral resolution (few nanometers instead of few hundred
49 from a RGB image). A spectrum for each pixel allows different post acquisition treatments
50 allowing separation of different contributors to the image at a pixel scale. Cesbron *et al.* [12]
51 proposed a method to simultaneously analyze dissolved iron and reactive phosphorous. This
52 is an excellent alternative to probes built with different layers of gel, [11] each one being
53 dedicated to one chemistry that need handling skills and do not guarantee a perfect match of
54 the different images (*i.e.*: distortion of the gel, gap between images).
55 As mentioned above, nitrate profiles obtained with gel techniques are limited by LOD of ion
56 chromatography and elution of gel into a solution that significantly dilutes chemicals. For this
57 reason, nitrite is rarely detected and only nitrate quantification can be done. The development
58 of a nitrate probe as a microelectrode by a Danish group in early 2000, [14,15] brought an
59 alternative to perform high-resolution profiling within the sediment at high-resolution (*ca.*;
60 100 μm). Despite an attempt of commercialization by Unisense, only researchers from the
61 original group were able to perform such profiles. Achieving high-resolution profiles of nitrite
62 and nitrate resolution, as shown by several authors, is of major importance to quantify benthic
63 diffusive fluxes and to investigate new reactional pathways for nitrogen transformations
64 within the sediment that is affected by bioturbation. However, at the scale of a
65 microenvironment (burrow wall, root apex, etc…), only multi-species high-resolution profiles
66 and/or 2D distribution can achieve correlations between chemical species despite high spatial
67 heterogeneity. The recent publication of a method of nitrate reduction using a solution of
68 vanadium chloride [16,17] allow us to examine the possibility to propose a colorimetric protocol
69 for simultaneous nitrite and nitrate determination combining gel sampling, colorimetry and a
70 2 dimensional image acquisition. Firstly, the present study aims to transpose the famous
71 Griess reaction[18] to gel technique in order to obtain a nitrite image of porewater in a
72 sedimentary setting at a sub-millimeter resolution. Secondly, we examine the possibility to

revisit the procedure using vanadium chloride as a nitrate reducer in order to achieve a nitrite/nitrate 2D probe that could successfully be deployed within the sediment.

2. Experimental section

2.1. Principle of the method

A polyacrylamide gel probe is prepared (polymerized, rinsed and degassed) and deployed within the sediment until diffusional equilibrium with porewater solutes (including NO_2^- and NO_3^-) is reached.

A first reagent gel is prepared, containing the Griess[18,19] reagent: the coloring reagent gel, allowing specifically the nitrite determination. A second reagent gel is prepared using vanadium chloride: the reducing reagent gel that reduces nitrate into nitrite, allowing nitrate determination. The probe gel is laid down onto the first coloring reagent gel in order to obtain an image of nitrite distribution as variations of pink coloration over the gel assemblage.

An imagery device allows the digitalization of the colored image (flatbed scanner for nitrite imagery alone, or hyperspectral camera for both nitrite and nitrate determinations).

In order to obtain the nitrate distribution over the gel, the reducing reagent gel is added to the two-layer assemblage after the first digitalization for nitrite. A second digitalization is operated on the three-layer assemblage and the subtraction of signals between both images is performed for each pixel in order to obtain the nitrate contribution over the gel probe.

2.2. Sampling gel preparation and deployment

The probe is a polyacrylamide hydrogel mounted on a polycarbonate plate (250 mm high, 150 mm wide and 3 mm thick). The plate has a central depression of 1 mm depth (180 × 97 mm, length × width) that holds the hydrogel keeping the probe tight.[12] The gel is maintained and protected from sediment by a PVDF hydrophilic membrane (0.2 µm, Durapore®) taped on the plate using a PVC adhesive tape (supporting information SI-1). The

gel is a polyacrylamide DET gel prepared according to Jézéquel *et al*.,[9] adapted from Zhang and Davison.[20] In brief, a mixture of acrylamide (30%, Roth), bisacrylamide (2%, Roth), TEMED (Roth) as a catalyzer and ammonium persulfate (APS; 1%, Sigma-Aldrich) as a polymerization initiator, is cast between two plates separated by a spacer. Polymerization occurred after *ca*. 15 min. at room temperature. The gel is rinsed and stored in deionized water (Millipore Milli-Q® system) until use. Before hydration, thickness of the gel is 0.92 mm but reaches about 1mm after 1h hydration. In order to avoid oxygen contamination of anoxic sediment during probe deployment, the probe is deoxygenated by nitrogen bubbling in deionized water (Millipore Milli-Q® system) at least 5 h before deployment. Probes were deployed into sediment for 5 hours allowing equilibration. [11]

2.3. Reagent gel preparation

Reagent gels are 0.46 mm-thick (0.5 mm after hydration), polyacrylamide hydrogels with the same composition as probe gels. [20] After polymerization, reagent gels are equilibrated during at least 30 min with 50 mL of a reagent solution in a plastic bag. The coloring reagent solution contains 0.07% sulfanilamide (Roth), 0.01 % N-1-naphthylethylenediamine dihydrochloride (NEDD) (Roth) and 0.14 % HCl (Roth) in Milli-Q® water (uncolored solution). The reducing reagent gel is equilibrated with 50 mL of a vanadium chloride solution (VCl_3 (Sigma Aldrich) 2.9 % (w/v), HCl 1.8 % (w/v) from a 30% suprapur acid (Roth)). This gel is colored green by the vanadium salt.

2.4. Standard gel preparation

The standard gel is prepared by diffusion of standard solutions into a 1-mm thick gel similar to the probe gel: [12] the gel is placed onto a *Plexiglas*® plate and covered by a second *Plexiglas*® plate with 7 circular wells (2.1 cm i.d.) drilled into it. Each well is equipped with a cylindrical tube representing a 5 mL vial when put onto the gel (the base of each cylinder

overhangs slightly from the Plexiglas® plate in order to be pressed onto the gel). The Plexiglas® plates are tightened together with 8 small clamps, ensuring sufficient pressure on the gel to avoid leakage of standard solutions. A volume of 3.5 mL of each standard solution was poured into a well and incubated during 1 h in order to ensure diffusive equilibration. Nitrate and nitrite standard solutions were prepared from $NaNO_3$ and $NaNO_2$ salts respectively (Fluka).

2.5. Gel assemblage mounting and colorimetric reaction

After equilibration, the coloring reagent gel is removed from the bag and quickly drained before being laid down onto a white plate. Residual drops are gently wiped and the probe gel is laid onto it. The whole assemblage is covered by a cellulose acetate film that protects against evaporation, then scanned after 15 min, the necessary time for the NEDD to react with nitrite and form the so-called pink Azo dye revealing the 2D nitrite distribution.

To reduce nitrate, the cellulose acetate film is carefully removed from the double layer gel assemblage (*i.e.*, probe + nitrite reagent gels) and a nitrate reducing gel is laid on top of it. The three-layer gel assemblage is then covered by a clean cellulose acetate film and incubated for 20 min in a 50°C oven under water-saturated atmosphere. This heating step is crucial for accelerating the kinetics of nitrate reduction. At that point, the produced nitrite has reacted with the Griess reagent and the three-layer gel can be scanned at its turn. The calibration gel is processed like the *in situ* gel probe.

Two calibration gels (one from nitrate solutions and one from nitrite solutions) are necessary for estimating the efficiency of nitrate reduction. In order to save time and guarantee comparable conditions, both nitrite and nitrate calibration gels (two strips) are laid side-by-side onto the same reagent gels to be processed together. We also recommend preparing a solution with both nitrate and nitrite for quality control. Solutions ranged between 1.5 and 40 µmol L^{-1} in either NO_2^- or NO_3^-. Linear range of the color intensity towards concentration can

be extended using thinner probe or standard gels (e.g., 0.5 instead of 1.0 mm). Hence, thinner gels reduce the optical path, resulting in weaker color intensities. As a consequence, the saturation concentration increases but LOD increases as well.

2.6. 2D imagery methods

2.6.1. Nitrite imagery from commercial flatbed scanner

To obtain only nitrite distribution, a commercial flatbed scanner (Canon Canoscan LiDE 600F) was used. From scanned images, intensity of colored zones of the 2D probe was processed by ImageJ® software. Images were decomposed into primary color intensities (red, green and blue (RGB), at about 100 nm wavelength resolution), each being converted to a gray-scale image [9]. The green color intensity was found to give the most sensitive response, since the nitrite-reagent compound (Azo dye) is pink.

2.6.2. Hyperspectral data acquisition and treatment for nitrite/nitrate mapping

This procedure does not require any specific equipment but does not allow simultaneous quantification of nitrite and nitrate because of the dark green coloration of the reducing reagent and its spectral signature prevents the pink Azo dye to be read. When simultaneous nitrate and nitrite distributions are sought, both nitrite and nitrite+nitrate images have to be obtained with a hyperspectral camera (here, a HySpex VNIR 1600) that has a sufficient wavelength resolution to separate signals coming from different layers of colored gel. The camera has 160 channels, covering the spectral range from 400 nm to 900 nm, with a spectral resolution of 4.5 nm and a sampling interval of 3.7 nm allowing the analysis of a continuing spectrum. The acquisition time was 2 minutes. The flat assembly gel probe + reactive complex + transparent film was laid down on a Spectralon® plate and then scanned in front of the camera and under controlled halogen light source. The camera was set up in the laboratory

to scan samples with square pixels providing a spatial resolution of about 190×190 µm per pixel (camera about 1m above samples).

According to Cesbron *et al.*,[12] reflectance spectra results of an intimate mixing of colored reagents within a transparent gel. Therefore it is possible to decompose each pixel into different end-members according to their spectra. The decomposition of each pixel is calculated as a linear combination of the logarithm of the different end-member spectra using ENVI® software (unmixing function). In the present study, 3 end-member spectra are considered: (1) the spectral background which corresponds to a Spectralon® plate + the two- or three-layer 2D gel (for respectively the first and the second scan); (2) a spectral nitrite end-member from the highest nitrite concentration of the calibration gel and (3) the spectrum corresponding to the vanadium(III) green coloration obtained from a nitrite-free part of the calibration gel. This unmixing procedure is applied to the calibration gel for signal linearity checking as concentration increases and to the probe gel for NO_2^- and VCl_3 signals separation.

2.7. Validation of the method

2.7.1. Validation of nitrite/nitrate separation

To ensure a complete separation of signal from nitrite and from nitrate, calibration standards were performed with two composite standards containing both species. The double standard gel (made of two strips, one for each chemical species) is laid onto the Griess reagent gel. At the first stage of the treatment, only the set of circles corresponding to the nitrite standard gel is supposed to turn pink. Obviously, the nitrite + nitrate composite circle would become as pink as its corresponding nitrite concentration enables it.

Once the assemblage is scanned by the hyperspectral camera, the VCl_3 reducing reagent gel is added and the new assemblage goes into the oven as described above (section 2.5). After 20 minutes, a new scanning is performed and reduced nitrate into nitrite appears pink. It is

193 important to note that the VCl_3 reducing reagent gel is dark green and low intensity pink is
194 not visible with naked eyes.
195 After unmixing calculation (section 2.4.), nitrite reflectance from both images can be achieved
196 (*i.e*. before and after addition of the dark green VCl_3 reducing agent gel). From the second
197 image (with the VCl_3 reducing reagent gel) a nitrite + newly produced nitrite image is
198 obtained. From the literature,[16] it is known that 20 min at 50°C is too short to achieve a
199 complete reduction but a longer incubation time will affect the distribution of nitrate because
200 of lateral diffusion (i.e., there is a competition between reduction kinetics and loss of signal
201 by diffusion, see section 3.1. and 3.2.). The comparison of standard curve slopes between
202 nitrite and nitrate standards allows quantifying the efficiency of nitrate reduction into nitrite
203 for each set of experiments and therefore calculation of nitrate concentration.
204 Summarizing, the first image is used for direct nitrite standardization while the second is used
205 to quantify nitrate reduction efficiency and therefore to quantify the sum of nitrite and the part
206 of nitrate that was reduced during the experience. The same two-step procedure is applied to
207 the probe gel.
208 The quantification of nitrite on the probe gel (two-layer gel) is for each pixel:
209
210 $[NO_2^-] = [(slope_{nitrite} \times R_{nitrite})$
211 where $slope_{nitrite}$ is the slope of the nitrite standard curve of the first image (without VCl_3 gel);
212 $R_{nitrite}$ is the reflectance of the assembled probe gel before addition of the VCl_3 gel.
213
214 The quantification of nitrate on the probe gel (three-layer gel) will be for each pixel:
215
216 $[NO_3^-] = [(slope_{nitrite}^{VCl3} \times R_{VCl3}) - [NO_2^-]] \times slope_{nitrite}^{VCl3}/slope_{nitrate}^{VCl3}$
217

where $slope_{nitrite}^{VCl3}$ is the slope of the nitrite standard curve of the second image (with VCl_3 gel); R_{VCl3} is the reflectance of the assembled probe gel after addition of the VCl_3 gel; $slope_{nitrate}^{VCl3}$ is the slope of the nitrate standard curve; $[NO_2^-]$ is the concentration of nitrite for each pixel after standardization of the assembled probe gel before addition of the VCl_3 gel.

2.7.2. Validation of the method for sediment

A series of laboratory experiments using estuarine sediment was realized in order to test the nitrite/nitrate method on more realistic conditions. Sediment was sampled in the Brillantes mudflat from the River Loire estuary (47°16'56.00"N 2° 3'47.00"W). The sediment is mainly composed of silt (92 %) with some clay (6 %) and sand (2 %) and is colonized in particular by microphytobenthic films (diatoms up to 60 mg m^{-2}; [21] and bioturbating macrofauna (mainly *Hediste diversicolor* and *Scrobicularia plana*; I. Metais, pers. comm.)

Laboratory experiment on homogenized sediment: sediment sampling occurred in June 2014. The sediment was sieved with a mesh of 1 mm in order to remove macrofauna. After homogenization, sediment was covered with estuarine water and left for equilibration for 12 days in the laboratory. Overlying water was constantly aerated and the system kept in the dark at room temperature until gel probes deployment. The day before deployment, a burrow was created using a 50 mL Falcon® tube and gently removed to keep the artificial burrow, and the probe was inserted in the axis of this artificial structure. Before retrieval of the probe, the surface water was sampled (about 5 cm above the sediment water interface, SWI) and nitrite was analyzed using the classical colorimetric technique with a spectrophotometer.

Laboratory experiment on a non-homogenized sediment: sediment sampling occurred in June 2015. This time, the sediment was neither sieved nor homogenized in order to maintain possible natural structures that could generate nitrite or nitrate microenvironments such as fecal pellets, dead organisms or burrows.

3. Results & Discussion

3.1. Colorimetric measurement of nitrite on a gel

3.1.1. Nitrite reaction characteristics

The first test of a protocol for colorimetric nitrite determination using gels consisted in simply starting from the well-known protocol of Griess,[18] modified for seawater by Bendschneider and Robinson [22] and detailed by Strickland and Parsons [23] and Grasshof *et al.* [24], adapting reagent proportions to gels. The superimposition of one coloring reagent gel with a thickness of *ca.* 0.5 mm to a probe gel with a thickness of 1 mm corresponds in a dilution with a ratio of 1/1.5 for nitrite from the sample gel and 1/3 for the chemicals from the reagent gel. The gels were prepared as described section 2. Figure 1 shows the successive images of the calibration gel *versus* time (Figure 1A) and the corresponding reflectance obtained with the commercial flatbed scanner (Figure 1B). The concentration of nitrite standards ranged from 1.25 to 40 µmol L^{-1}. Coloration clearly appears after 2 min. However, below 5 µmol L^{-1} it appears difficult to distinguish nitrite signal with naked eyes and it is necessary to perform a numerical treatment (*e.g.* with ImageJ® densitometry software). Once it is done, the differences between the standards and the background are significant down to a concentration of 1.25 µmol L^{-1}. The time series lasting over 96 min indicates that the colorimetric reaction is complete 10 min after contact between the reagent gel and the calibration gel. This supports the idea that the kinetics of colorimetric reaction is similar to classical spectroscopic measurements and in a gel assemblage (see references above).

Figure 1C shows the evolution of a coloration profile across the edge of the 19.5 µmol L^{-1} nitrite standard-well according to time. The good superimposition of profiles within the time-series indicates that no diffusion seems to take place laterally after contact between the calibration gel and the reagent gel. In particular, there is no visible relaxation of gradient concentration during the colorimetric reaction. However, the asymptotic diffusive profile

268 centered at the limit of the well, that held the standard solution, seems to indicate that during
269 the equilibrium step between the standard solutions and the calibration gel, nitrite is free to
270 diffuse laterally beyond the well limits. Similar observations were made for iron and
271 phosphorous previously. [12] These results indicate that the colored component has a much
272 slower diffusion coefficient than the free nitrite. It also suggests that the time of relaxation of
273 the signal by lateral diffusion of solutes in the gel during handling (i.e. from time of probe
274 retrieving to coloration process), is a crucial parameter that strongly limits the maximal
275 resolution of this method and special care must be taken while interpreting sub-millimeter 2D
276 structures. [12,25]
277 Since the signal does not evolve significantly after 10 minutes, the maximum reflectance
278 intensity can be correlated with standard concentrations to realize a standard curve
279 (coefficient of determination of 0.9972). The standard curve allows calculating a limit of
280 detection (3-fold standard error of the blank) of 1.7 µmol L^{-1} and a limit of quantification
281 (LOQ) about 5 µmol L^{-1} (10-fold standard error of the blank). Accuracy is about 2 µmol L^{-1}
282 within the range from 0 to 40 µmol L^{-1}.

283 **3.1.2. Application on a homogenized sediment**

284 Figure 2 shows the two-dimensional distribution of nitrite obtained after deployment of a gel
285 probe within the sieved sediment that was artificially perturbed. The overall feature of the
286 nitrite distribution seems to follow the shape of the perturbation with concentration up to
287 15 µmol L^{-1}. The image shows that nitrite concentrations ranged between 10 and 15 µmol L^{-1}
288 in the first centimeter above the SWI. A water sample taken 5 cm above (near the air-water
289 interface), and analyzed classically (with a spectrophotometer), showed a concentration of 5.8
290 µmol L^{-1} suggesting a nitrite flux from the sediment into the overlying water of the aquarium.
291 As expected, below 2 cm depth (and around the artificial burrow), nitrite is depleted reaching

LOD at 5 cm depth, likely by denitrification or anammox processes occurring in the sediment [26] or abiotically due to lower redox potential.

The first goal of this paper was to transpose the classical nitrite colorimetric determination to a 2D gel in order to describe nitrite distribution at high resolution affected by any sedimentary structure. The results shown here indicate that this goal was achieved.

3.2. Simultaneous nitrite and nitrate 2D analysis

3.2.1. Optimization of nitrate reduction kinetics

The recent publications [16,17] considering the use of a vanadium chloride solution instead of the widely used granular copperized cadmium column for nitrate reduction to nitrite [27] brought new perspectives for the applicability of a colorimetric technique for nitrate in gels. However, there is a major limitation in the transposition of the protocols established by these studies to gel imagery: the slow kinetics of nitrate reduction into nitrite. Hence, a slow colorimetrical reaction would favor relaxation of strong concentration gradients by diffusion of nitrate before immobilization by colorimetrical reaction. To keep the ability of the 2D DET to catch millimeter features in sediment it is necessary to optimize the kinetics of nitrate reduction with VCl_3. Schnetger and Lehners (2014) established that a complete reduction of nitrate into nitrite with VCl_3 takes 10 hours at ambient temperature and 40 min at 45°C using a 0.57 % (w/v) VCl_3 reagent solution.[16] Similar results were found by Garcia-Robledo *et al*. (2014). In addition, García-Robledo *et al*. showed that kinetics is also dependent of the concentration of vanadium and of the acidity of the reducing reagent.[17] At 50°C, they showed that time of nitrate reduction decreases by more than a half when VCl_3 increases from 0.5 to 2 % (w/v). A similar experiment was realized in the present study (see supporting information, SI-2) that showed that for a VCl_3 concentration of 0.017 mol L^{-1} (Schnetger and Lehners recipe) [16] at 30°C, 100% of nitrate was reduced after 2 h and only 45 min was needed with 0.07 mol L^{-1}. Therefore it is possible to apply this nitrate reduction technique to 2D DET nitrate imagery

317 accepting a relaxation effect during 45 min *i. e.* of about roughly 2 mm (in all directions)
318 which is not ideal for a sub-millimeter resolution image.

319 **3.2.2. Hyperspectral analysis: accuracy and LOD improvements**

320 Use of the vanadium chloride solution (a dark green solution) creates a second problem as the
321 solution absorbs a certain quantity of light with a particular spectral signature and therefore is
322 likely to raise the LOD of the 2D DET nitrate imagery. Preliminary tests performed with
323 commercial flatbed scanner showed that VCl_3 (at 0.07 mol L^{-1}) interferences prevent the
324 detection of nitrate. Further investigation revealed that the hyperspectral camera allows
325 detecting nitrate (despite 0.07 mol L^{-1} of VCl_3) but only above 10 µmol L^{-1}. As shown in the
326 spectra described in the supporting information (SI-3), accuracy of nitrite detection is
327 constrained by the absorption band of the complex coloring reagent + probe + reducing
328 reagent gels between 450 nm and 590 nm. However, the adjunction of a dark green vanadium
329 chloride gel considerably modifies the background. The signal brought by vanadium(III)
330 (between 490 and 660 nm) is spread over the entire visible spectrum including where the
331 nitrite peak develops. To overcome this limitation and keep acceptable reduction kinetics we
332 chose to work with a final concentration of VCl_3 = 0.035 mol L^{-1} in the reducing reagent gel,
333 with a time span for nitrate reduction of 20 min at the temperature of 50°C.
334 Standard curves obtained for nitrite and nitrate (SI-4) with the optimized protocol for an
335 assemblage of coloring reagent+calibration+reducing reagent gels show good linearity (r^2 =
336 0.996 and 0.989 for nitrite and nitrate respectively) with a LOD about 1.7 µmol L^{-1} (3-fold
337 standard deviation of the blank reflectance), a 5 µmol L^{-1} LOQ and a 2 µmol L^{-1} accuracy. By
338 analogy with length of cuvettes, thickening the probe gel increases reflectance and therefore
339 would allow LOD increasing if necessary. However, a thicker gel requires an increase of in
340 situ deployment time and results in a decreasing of spatial definition of 2D structures because
341 of lateral diffusion within the gel. [25]

342 The comparison of nitrite and nitrate standard curves allows the determination of an averaged
343 nitrate reduction efficiency by comparison of slopes. A 100% nitrate reduction rate would
344 lead to a $slope_{nitrate}/slope_{nitrite}$ equal to 1. Standard curve for nitrate has a slope of 0.0450 (SI-4)
345 while the standard curve for nitrite has a slope of 0.0501; the ratio indicates a nitrate reduction
346 efficiency of about 90%. Once, the quantification of nitrate reduction efficiency determined, it
347 is possible to quantify the nitrate concentration within the gel despite the lack of a total
348 reduction of nitrate. Another experiment was realized with slightly different conditions
349 (reduction time of 10 minutes and temperature of 40°C) that gave a nitrate reduction
350 efficiency of about 75%. These results suggest that the interplay between nitrate reduction
351 kinetics and diffusion smoothing of 2D structures has to be considered carefully while
352 biogeochemical interpretations about microniches or other sedimentary structures are
353 hypothesized. A simple transport modeling shows that if only diffusion governs nitrate
354 transportation within a gel, a production layer will vertically spread over twice its thickness
355 after 40 mn at 50°C (see details in SI-5). This means that a very precise knowledge about
356 diffusion of chemical species within the gel at different temperatures and for each step of the
357 colorimetric protocol has to be acquired for good modeling of signal relaxation and therefore
358 2D structure reconstruction. A more empiric approach was chosen to evaluate such relaxation
359 in the section 3.1.1 for nitrite. Results suggest that, once the pink azo dye is formed, diffusion
360 is greatly slowed down and cannot be observed within the time of the experiment. During the
361 second step of the protocol (nitrate reduction using VCl_3), nitrate can diffuse and signal be
362 relaxed since the Griess reaction did not occur yet. Our results suggest that at a millimeter
363 scale, this would not significantly affect structure shapes but probably affect more chemical
364 gradients across their edges.

3.2.3. Application on an incubated sediment

Unlike the nitrite testing (section 3.1), this experiment used sediment unsieved and non-homogenized in order to keep potential sedimentary or biogenic structures. Figure 3 shows the distribution of nitrite obtained from the first scan (*i.e.* first reagent gel over the probe gel) in the left panel and nitrite + reduced nitrate from the second scan in the central panel. Efficiency of nitrate reduction was taken as 90% according to the standardization. The right panel shows the resulting nitrate distribution after nitrite subtraction and efficiency correction. Nitrite remains below 5 µmol L^{-1} over the 15 cm of the gel inserted into the sediment while nitrate shows maximal concentrations over 40 µmol L^{-1} near the SWI. Despite lateral heterogeneity, nitrate seems to decrease below the LOD at 4 cm depth. One can note a spherical patch about 13 cm below the SWI.

Figure 4 and Figure 5 show separately nitrite and nitrate 2D distribution respectively extracted from Figure 3 with appropriate rescaling. Vertical lines over the picture correspond to profile extractions shown in right panels. The three nitrite profiles are very similar suggesting little lateral variability. Near the SWI, nitrite concentration is about 6 µmol L^{-1}. There is a decrease to a minimum of ~2 µmol L^{-1} at 4 cm depth. Below, nitrite concentration remains roughly constant between LOD and LOQ (limit of quantification). Nitrate profiles show a more complex pattern (Figure 5). All profiles show a nitrate maximum approximately 1 cm below the SWI indicating nitrification. [26,28] Then nitrate reaches zero at 5 cm depth. Below 10 cm depth, nitrate seems to be stable at a concentration below LOD. The variability of maximum intensities that ranges between 20 and 40 µmol L^{-1} illustrates the high lateral variability of such sediment at a millimeter scale. Such a variability is visible as well for dissolved iron and phosphorus for *in situ* deployments in the same area [13] mostly explained by the presence of active burrows of polychaetes.

The lateral variability of nitrate gradients intensity below the SWI highlights the importance of bioturbation for nitrogen cycling [29–32] and especially for oxidation of ammonium and nitrate release from sediment into water column. Bioturbation can enhance nitrate consumption producing N_2O and/or N_2 by denitrification or by oxydation of reduced compounds such as FeS or Fe^{2+}, [33] or producing again ammonium by dissimilatory nitrate reduction to ammonium (DNRA). This is of major importance considering the fact that nutrient availability controls benthic primary production and that microphytobenthic mats play an important role on the food web and on stabilization of the sedimentary substratum. [34] Important nitrate production would also imply reduction of oxidizers such as manganese and iron oxy(hydroxi)des and therefore enhancement of metal remobilization and recycling. [33,35,36] Therefore, we offer here the possibility to examine in 2 dimensions, the spatial nitrite and nitrate variability at a sufficient resolution that allows to describe chemical gradients generated by a mm-sized dead organism, a root apex, along a burrow wall. Further, these processes could be quantified with appropriate modeling. [37,38] Indeed, a double layer gel can be performed to sample at the same location both nitrite/nitrate and iron/phosphate couples. The image of nitrate distribution shows microenvironments at subsurface, between the oxic zone and the iron remobilization zone, and more surprisingly 13 cm below the interface suggesting that noisy profiles in the literature, that are often obtained from core slicing could not be artifacts but could be a result of the sampling of a microenvironment similar to the one shown here that peaks at about 30 $\mu mol\ L^{-1}$.

Combining colorimetry, gel sampling and hyperspectral imagery allows assessing, at sub-millimeter resolution in 2 dimensions, nitrite and nitrate production/consumption hotspots within a range between 1 and 40 $\mu mol\ L^{-1}$ without sampling discretization. However, due to relaxation effects, fidelity of concentration is achieved at a millimeter resolution. This technique is a good alternative to microsensors that allow sub-millimeter profiling but are difficult to perform and time-consuming as several profiles are needed to assess 2D

416 distribution (at a low resolution anyway). The protocol proposed here allowed to describe
417 nitrate release as microniches below the "zero-nitrate" layer and to evidence the lateral
418 variability of nitrate concentration in estuarine muddy sediment. Such technique offers
419 numerous perspectives for laboratory and *in situ* studies dealing with the reactivity of
420 microenvironments such as burrows or decaying macro(meio)fauna locations. Combined to
421 other high-resolution 2D analyses such as Fe/PO_4 gels, this method will provide valuable
422 insights on the mechanisms that control nutrient release and primary production feedback.

423 **4. Acknowledgements**

424 This study is part of the RS2E – OSUNA project funded by the Région Pays de la Loire.
425 Thanks to Romain Levrard, Livia Defaye and Manuel Giraud for their technical help.
426

427 **Supporting information**

428 Supporting information shows a scheme of the probe gel (SI-1); the kinetics of nitrate
429 reduction into nitrite as a function of vanadium chloride concentration (SI-2); different spectra
430 of reflectance obtained with a hyperspectral camera for the gels at different stages of
431 processing (SI-3); standard curves for nitrite and nitrate that allows to quantify reducing
432 efficiency fo nitrate into nitrite (SI-4); and the theoretical relaxation of a nitrate peak after gel
433 processing considering molecular diffusion (SI-5). This information is available free of charge
434 via the Internet at http://pubs.acs.org/ .
435

436 **Figure caption**
437

438 Figure 1: kinetics of nitrite colorimetric reaction on a gel. A: color evolution of the standard
439 curve over time. B: extracted reflectance (green channel) from images. C: overtime profile
440 evolution across the edge of a well (black line on the images (A); 19.5 µmol L^{-1} NO_2^-)
441 Figure 2: 2D nitrite concentration distribution and examples of selected profiles for a sieved
442 and homogenized sediment of the Brillantes mudflat Loire estuary, artificially "bioturbated"
443 by a 3 cm-diameter tube. Dots are data and lines are smoothed profiles.
444 Figure 3: 2D nitrite (left), nitrite + reduced nitrate (middle), calculated nitrate (right) for an
445 incubated sediment from the Brillantes mudflat, Loire estuary
446 Figure 4: 2D nitrite distribution (left) extracted from Figure 3 and rescaled, and examples of
447 selected profiles for incubated sediment of the Brillantes mudflat, Loire estuary. Dots are data
448 and lines smoothed profiles.
449 Figure 5: 2D nitrate distribution (left) extracted from Figure 3, and examples of selected
450 profiles for an incubated sediment of the Brillantes mudflat, Loire estuary. Dots are data and
451 lines smoothed profiles.
452

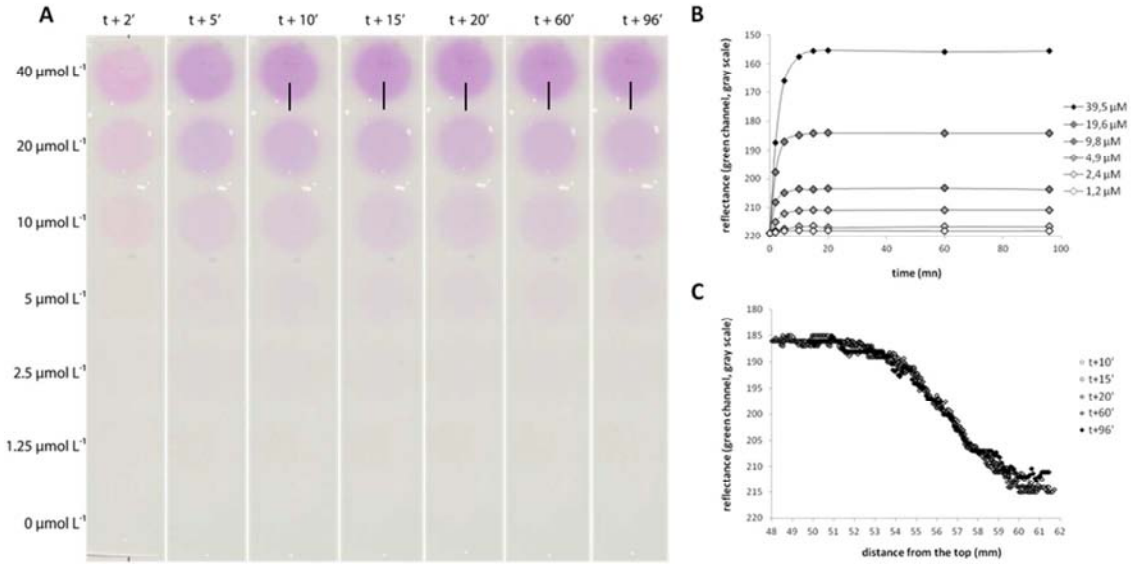

Figure 1: kinetics of nitrite colorimetric reaction on a gel. A: color evolution of the standard curve over time. B: extracted reflectance (green channel) from images. C: overtime profile evolution across the edge of a well (black line on the images (A); 19.5 µmol L^{-1} NO_2^-)

460

461

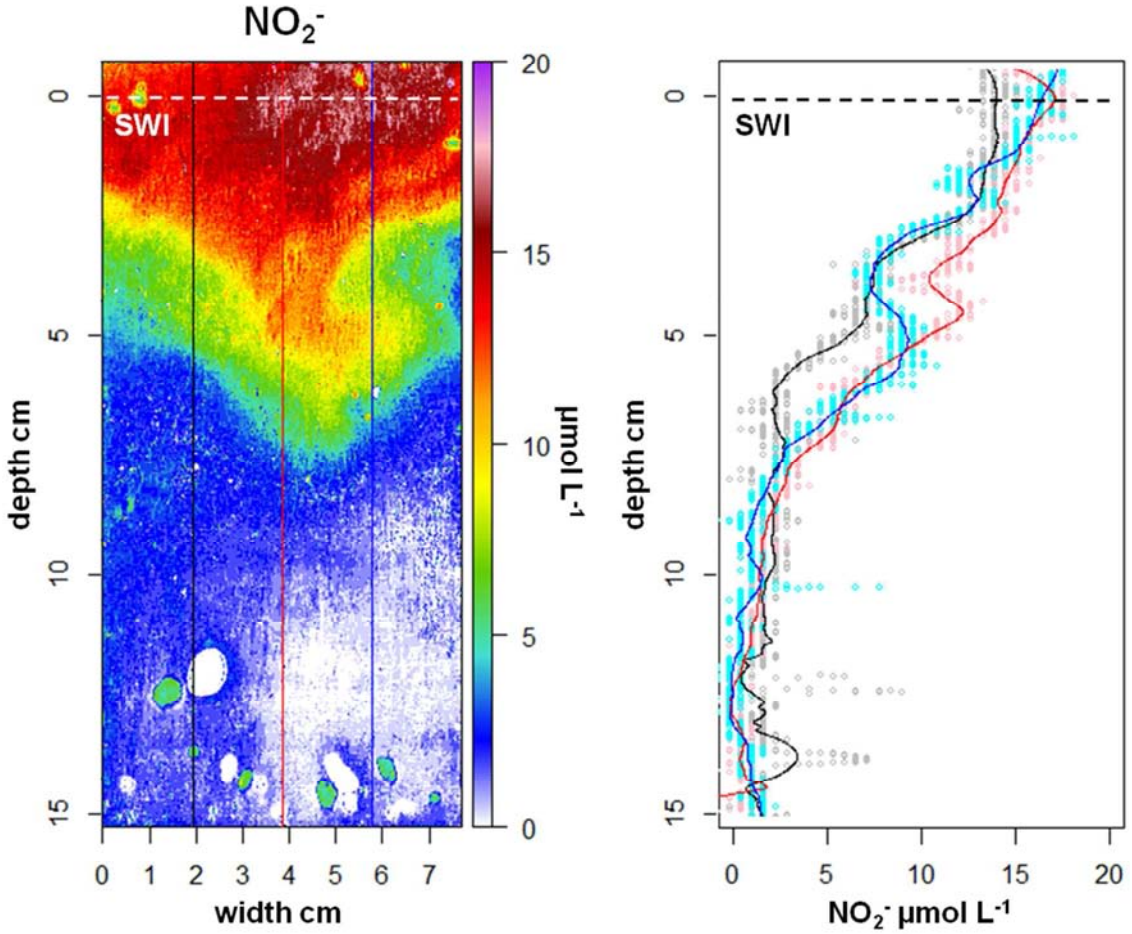

462

463 **Figure 2: 2D nitrite concentration distribution and examples of selected profiles for a sieved and homogenized**
464 **sediment of the Brillantes mudflat Loire estuary, artificially "bioturbated" by a 3 cm-diameter tube. Dots are data**
465 **and lines are smoothed profiles.**

466

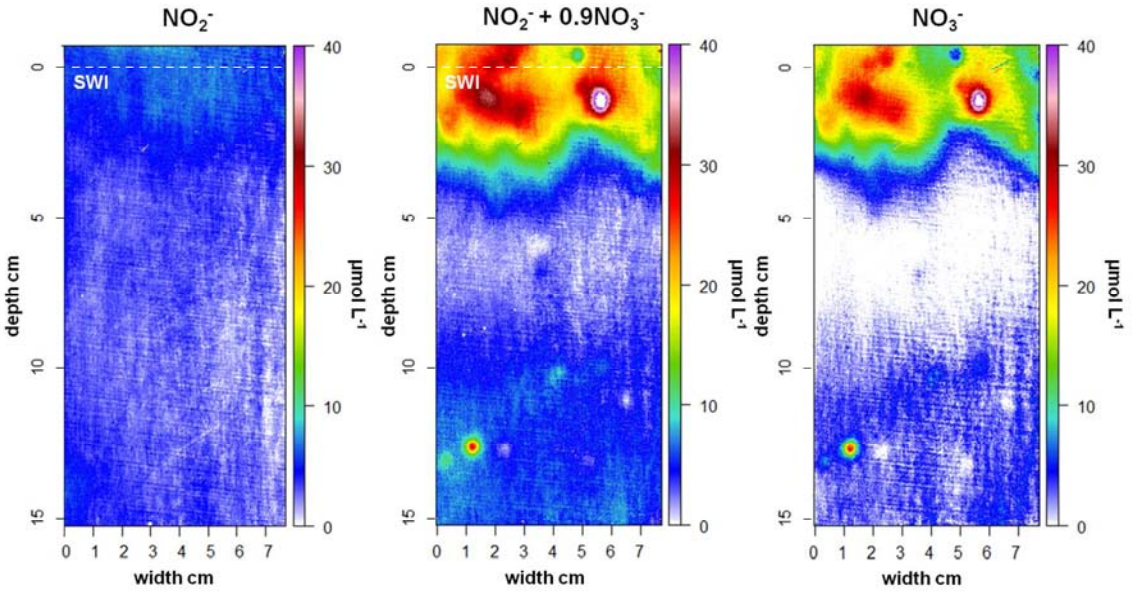

Figure 3: 2D nitrite (left), nitrite + reduced nitrate (middle), calculated nitrate (right) for an incubated sediment from the Brillantes mudflat, Loire estuary

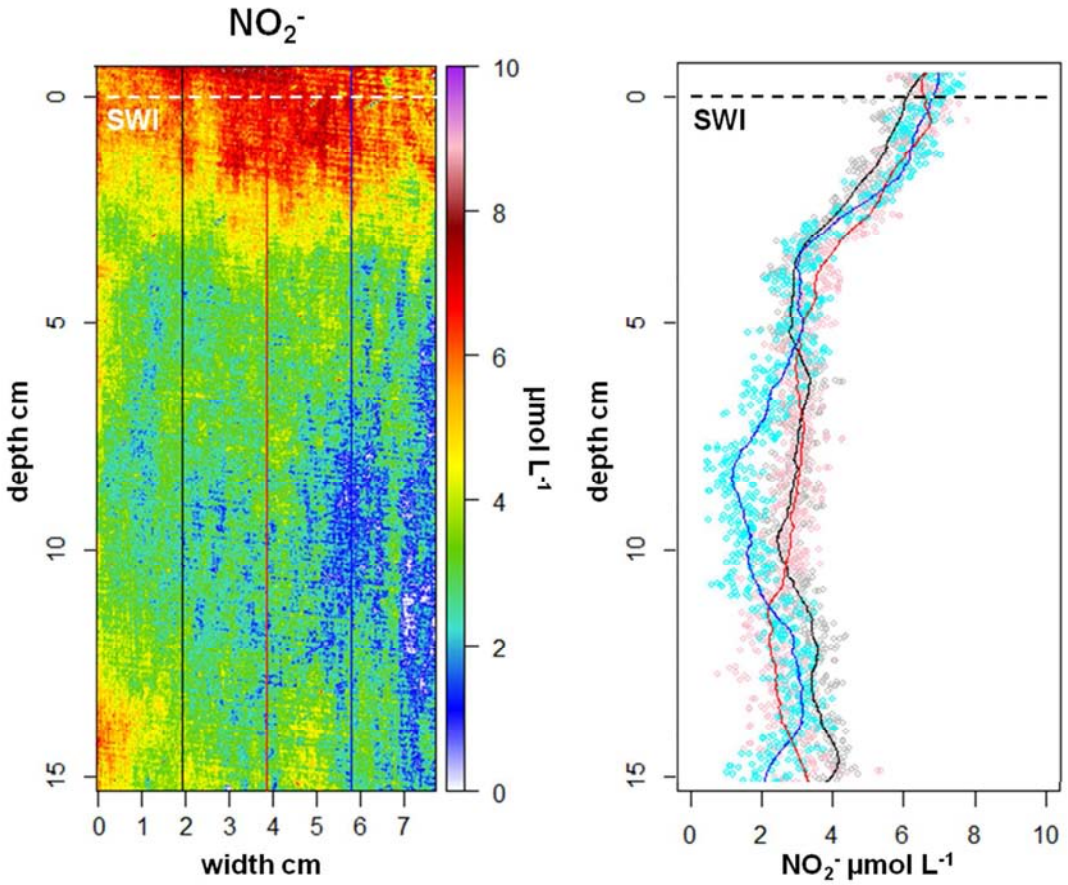

Figure 4: 2D nitrite distribution (left) extracted from Figure 3 and rescaled, and examples of selected profiles for incubated sediment of the Brillantes mudflat, Loire estuary. Dots are data and lines smoothed profiles.

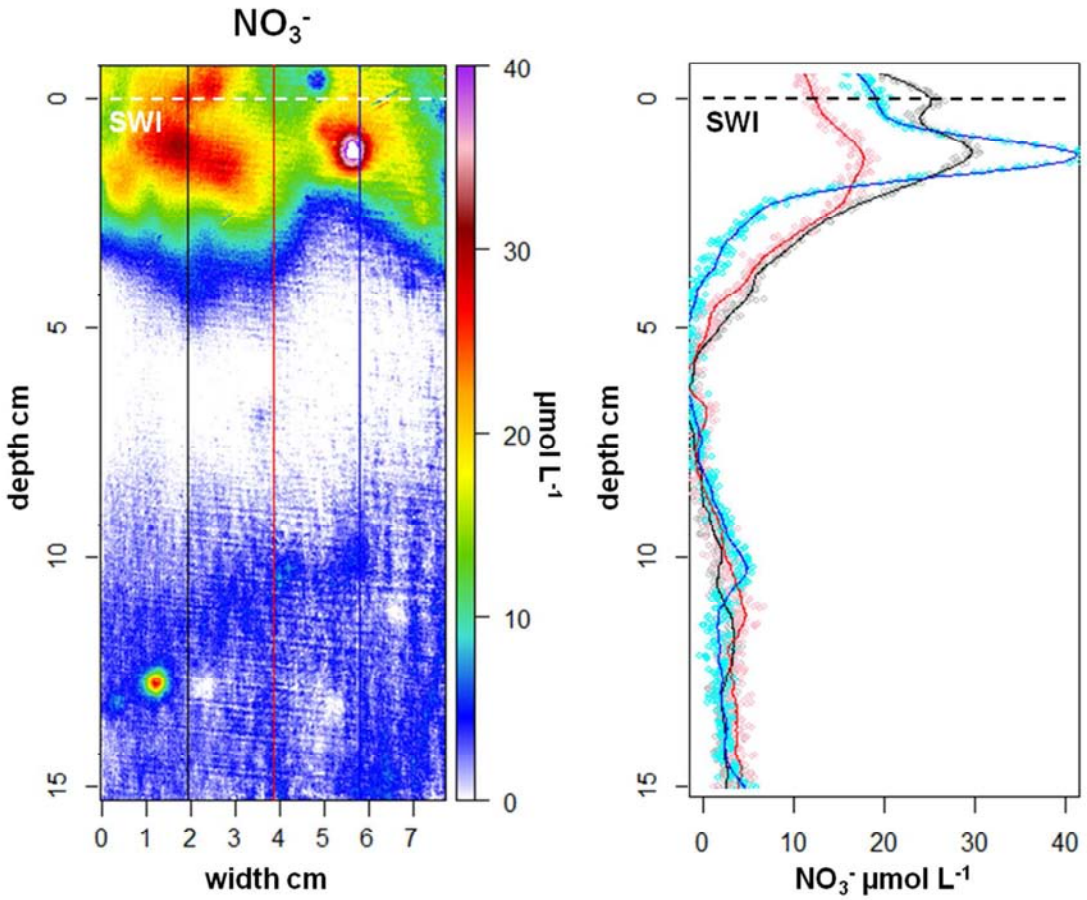

Figure 5: 2D nitrate distribution (left) extracted from Figure 3, and examples of selected profiles for an incubated sediment of the Brillantes mudflat, Loire estuary. Dots are data and lines smoothed profiles.

References

(1) Davison, W.; Grime, G. W.; Morgan, J. a. W.; Clarke, K. Distribution of dissolved iron in sediment pore waters at submillimetre resolution. *Nature* **1991**, *352* (6333), 323–325.

(2) Monbet, P.; McKelvie, I. D.; Worsfold, P. J. Combined Gel Probes for the In Situ Determination of Dissolved Reactive Phosphorus in Porewaters and Characterization of Sediment Reactivity. *Environ. Sci. Technol.* **2008**, *42* (14), 5112–5117.

(3) Koschorreck, M.; Brookland, I.; Matthias, A. Biogeochemistry of the sediment–water interface in the littoral of an acidic mining lake studied with microsensors and gel-probes. *J. Exp. Mar. Biol. Ecol.* **2003**, *285–286*, 71–84.

(4) Metzger, E.; Viollier, E.; Simonucci, C.; Prévot, F.; Langlet, D.; Jézéquel, D. Millimeter-scale alkalinity measurement in marine sediment using DET probes and colorimetric determination. *Water Res.* **2013**, *47* (15), 5575–5583.

(5) Stockdale, A.; Davison, W.; Zhang, H. Micro-scale biogeochemical heterogeneity in sediments: A review of available technology and observed evidence. *Earth-Sci. Rev.* **2009**, *92* (1–2), 81–97.

(6) Shuttleworth, S. M.; Davison, W.; Hamilton-Taylor, J. Two-Dimensional and Fine Structure in the Concentrations of Iron and Manganese in Sediment Pore-Waters. *Environ. Sci. Technol.* **1999**, *33* (23), 4169–4175.

(7) Krause, S.; Tecklenburg, C.; Munz, M.; Naden, E. Streambed nitrogen cycling beyond the hyporheic zone: Flow controls on horizontal patterns and depth distribution of nitrate and dissolved oxygen in the upwelling groundwater of a lowland river. *J. Geophys. Res. Biogeosciences* **2013**, *118* (1), 54–67.

(8) Mortimer, R. J. G.; Krom, M. D.; Harris, S. J.; Hayes, P. J.; Davies, I. M.; Davison, W.; Zhang, H. Evidence for suboxic nitrification in recent marine sediments. *Mar. Ecol. Prog. Ser.* **2002**, *236* (1), 31–35.

(9) Jézéquel, D.; Brayner, R.; Metzger, E.; Viollier, E.; Prévot, F.; Fiévet, F. Two-dimensional determination of dissolved iron and sulfur species in marine sediment pore-waters by thin-film based imaging. Thau lagoon (France). *Estuar. Coast. Shelf Sci.* **2007**, *72* (3), 420–431.

(10) Robertson, D.; Teasdale, P. R.; Welsh, D. T. A novel gel-based technique for the high resolution, two-dimensional determination of iron (II) and sulfide in sediment. *Limnol. Oceanogr. Methods* **2008**, *6* (10), 502–512.

(11) Pagès, A.; Teasdale, P. R.; Robertson, D.; Bennett, W. W.; Schäfer, J.; Welsh, D. T. Representative measurement of two-dimensional reactive phosphate distributions and co-distributed iron(II) and sulfide in seagrass sediment porewaters. *Chemosphere* **2011**, *85* (8), 1256–1261.

(12) Cesbron, F.; Metzger, E.; Launeau, P.; Deflandre, B.; Delgard, M.-L.; Thibault de Chanvalon, A.; Geslin, E.; Anschutz, P.; Jézéquel, D. Simultaneous 2D Imaging of Dissolved Iron and Reactive Phosphorus in Sediment Porewaters by Thin-Film and Hyperspectral Methods. *Environ. Sci. Technol.* **2014**, *48* (5), 2816–2826.

(13) Thibault de Chanvalon, A.; Metzger, E.; Mouret, A.; Cesbron, F.; Knoery, J.; Rozuel, E.; Launeau, P.; Nardelli, M. P.; Jorissen, F. J.; Geslin, E. Two-dimensional distribution of living benthic foraminifera in anoxic sediment layers of an estuarine mudflat (Loire estuary, France). *Biogeosciences* **2015**, *12* (20), 6219–6234.

(14) Larsen, L. H.; Damgaard, L. R.; Kjær, T.; Stenstrøm, T.; Lynggaard-Jensen, A.; Revsbech, N. P. Fast responding biosensor for on-line determination of nitrate/nitrite in activated sludge. *Water Res.* **2000**, *34* (9), 2463–2468.

(15) Revsbech, N. P.; Glud, R. N. Biosensor for laboratory and lander-based analysis of benthic nitrate plus nitrite distribution in marine environments. *Limnol. Oceanogr. Methods* **2009**, *7* (11), 761–770.

(16) Schnetger, B.; Lehners, C. Determination of nitrate plus nitrite in small volume marine water samples using vanadium(III)chloride as a reduction agent. *Mar. Chem.* **2014**, *160*, 91–98.

(17) García-Robledo, E.; Corzo, A.; Papaspyrou, S. A fast and direct spectrophotometric method for the sequential determination of nitrate and nitrite at low concentrations in small volumes. *Mar. Chem.* **2014**, *162*, 30–36.

(18) Griess, P. Bemerkungen zu der Abhandlung der HH. Weselsky und Benedikt „Ueber einige Azoverbindungen”. *Berichte Dtsch. Chem. Ges.* **1879**, *12* (1), 426–428.

(19) Bratton, A. C.; Marshall, E. K.; Hendrickson, W. the technical assistance of D. B. and A. R. A New Coupling Component for Sulfanilamide Determination. *J. Biol. Chem.* **1939**, *128* (2), 537–550.

(20) Zhang, H.; Davison, W. Diffusional characteristics of hydrogels used in DGT and DET techniques. *Anal. Chim. Acta* **1999**, *398* (2), 329–340.

(21) Benyoucef, I.; Blandin, E.; Lerouxel, A.; Jesus, B.; Rosa, P.; Méléder, V.; Launeau, P.; Barillé, L. Microphytobenthos interannual variations in a north-European estuary (Loire estuary, France) detected by visible-infrared multispectral remote sensing. *Estuar. Coast. Shelf Sci.* **2014**, *136*, 43–52.

(22) Bendschneider, K.; R J Robinson. A new spectrophotometric method for determination of nitrite in sea water. *J. Mar. Res.* **1952**, *11*, 87–96.

(23) Strickland, J. D. H.; Parsons, T. R. *A practical handbook of seawater analysis*; Fisheries Research Board of Canada, 1972.

(24) Grasshoff, K.; Kremling, K.; Ehrhardt, M. *Methods of Seawater Analysis*; John Wiley & Sons, 2009.

(25) Harper, M. P.; Davison, W.; Tych, W. Temporal, Spatial, and Resolution Constraints for in Situ Sampling Devices Using Diffusional Equilibration: Dialysis and DET. *Environ. Sci. Technol.* **1997**, *31* (11), 3110–3119.

(26) Burgin, A. J.; Hamilton, S. K. Have we overemphasized the role of denitrification in aquatic ecosystems? A review of nitrate removal pathways. *Front. Ecol. Environ.* **2007**, *5* (2), 89–96.

(27) Wood, E. D.; Armstrong, F. a. J.; Richards, F. A. Determination of nitrate in sea water by cadmium-copper reduction to nitrite. *J. Mar. Biol. Assoc. U. K.* **1967**, *47* (1), 23–31.

(28) Sørensen, J.; Jørgensen, B. B.; Revsbech, N. P. A comparison of oxygen, nitrate, and sulfate respiration in coastal marine sediments. *Microb. Ecol.* **1979**, *5* (2), 105–115.

(29) Aller, R. C.; Aller, J. Y. The effect of biogenic irrigation intensity and solute exchange on diagenetic reaction rates in marine sediments. *J. Mar. Res.* **1998**, *56* (4), 905–936.

(30) Bonaglia, S.; Nascimento, F. J. A.; Bartoli, M.; Klawonn, I.; Brüchert, V. Meiofauna increases bacterial denitrification in marine sediments. *Nat. Commun.* **2014**, *5*, 5133.

(31) Gilbert, F.; Aller, R. C.; Hulth, S. The influence of macrofaunal burrow spacing and diffusive scaling on sedimentary nitrification and denitrification: An experimental simulation and model approach. *J. Mar. Res.* **2003**, *61* (1), 101–125.

(32) Stief, P. Stimulation of microbial nitrogen cycling in aquatic ecosystems by benthic macrofauna: mechanisms and environmental implications. *Biogeosciences* **2013**, *10* (12), 7829–7846.

(33) Hulth, S.; Aller, R. C.; Gilbert, F. Coupled anoxic nitrification/manganese reduction in marine sediments. *Geochim. Cosmochim. Acta* **1999**, *63* (1), 49–66.

(34) MacIntyre, H. L.; Geider, R. J.; Miller, D. C. Microphytobenthos: The ecological role of the “secret garden” of unvegetated, shallow-water marine habitats. I. Distribution, abundance and primary production. *Estuaries* **1996**, *19* (2), 186–201.

(35) Anschutz, P.; Zhong, S.; Sundby, B.; Mucci, A.; Gobeil, C. Burial efficiency of phosphorus and the geochemistry of iron in continental margin sediments. *Limnol. Oceanogr.* **1998**, *43* (1), 53–64.

(36) Fernandes, S. O.; Javanaud, C.; Aigle, A.; Michotey, V. D.; Guasco, S.; Deborde, J.; Deflandre, B.; Anschutz, P.; Bonin, P. C. Anaerobic nitrification–denitrification mediated by Mn-oxides in meso-tidal sediments: Implications for N2 and N2O production. *J. Mar. Syst.* **2015**, *144*, 1–8.

(37) Zhu, Q.; Aller, R. C.; Fan, Y. Two-dimensional pH distributions and dynamics in bioturbated marine sediments. *Geochim. Cosmochim. Acta* **2006**, *70* (19), 4933–4949.

592 (38) Thibault de Chanvalon, A.; Metzger, E.; Mouret, A.; Geslin, E.; Knoery, J.; Meysman,
593 F. J. R. Two dimensional mapping of iron release in marine sediments at submillimetre
594 scale. *Mar. Chem.* **in press**.
595